

IMECE2022/95456

MODELING THE BURNING OF POLYMER MATRIX: TRAINING COLLOCATION PHYSICS-INFORMED NEURAL NETWORK

Aref Ghaderi

Department of Civil & Env. Eng.
Michigan State University
East Lansing, Michigan 48824
Email: ghaderi1@msu.edu

Roozbeh Dargazany*

Department of Civil & Env. Eng.
Michigan State University
East Lansing, Michigan 48824
Email: roozbeh@msu.edu

ABSTRACT

The combined impacts of thermal, chemical, and physical processes play a significant role in the pyrolysis problems in polymeric materials. Thermal energy is transported into the material via thermal convection when the charring materials are subjected to high-temperature loading. Decomposition of the resin will result in pyrolytic gases and solid leftovers. The material can be split into three zones based on the degree of pyrolysis of the material: (i) charring zone, in which the material entirely decomposes; (ii) pyrolysis zone, in which the material is disintegrating; and (iii) virgin material zone, in which the material has not yet begun to decompose. Physics-informed neural networks (PINNs) are neural networks whose components contain model equations, such as partial differential equations (PDEs). A multi-task learning approach has emerged in which a NN must fit observed data while decreasing a PDE residual. This article introduces PINN architectures to forecast temperature distributions and the degree of burning of a pyrolysis problem in a one-dimensional (1D) and two-dimensional (2D) rectangular domain. The complex, non-convex multi-objective loss function presents substantial obstacles for forward problems in training PINNs. We discovered that adding several differential relations to the loss function causes an unstable optimization issue, which may lead to convergence to the trivial null solution or significant deviation of the solution. To address this problem, the dimensionless form of the coupled governing equations that we find most beneficial to the optimizer is used. The numerical results

are compared with results obtained from PINN to show the performance of the solution. Our research is the first to explore fully coupled temperature-degree-of-burning relationships in pyrolysis problems. Unlike classical numerical methods, the proposed PINN does not depend on domain discretization. In addition to these characteristics, the proposed PINN achieves good accuracy in predicting solution variables, which makes it a candidate to be utilized for surrogate modeling of pyrolysis problems. In summary, the pyrolysis model of materials is solved with the PINN framework; We assumed that all thermal properties of a material (thermal conductivity, specific heat, and density) are affected by temperature and degree of burning. While the achieved results are close to our expectations, it should be noted that training PINNs is time-consuming. We relate the training challenge to the multi-objective optimization issue and the application of a first-order optimization algorithm, as reported by others. Given the difficulties encountered and overcome in this work for the forward problem, the next step is to use PINNs to inverse burning situations.

INTRODUCTION

Pyrolysis is one of the many different types of chemical decomposition processes that take place at higher temperatures. It differs from other processes like combustion and hydrolysis in that it seldom requires the addition of additional reagents such as oxygen (O_2) or water (in hydrolysis). Pyrolysis results in solids (char), condensable liquids (tar), and non-condensing/permanent

*Address all correspondence to this author.

gases [1, 2]. Pyrolysis is widely used in the chemical industry to make ethylene, various kinds of carbon, and other compounds from petroleum, coal, and even wood, as well as to make coal coke.

Before getting into the details of the models, it is crucial to understand what happens when the polymer is exposed to a high-temperature heat source. When organic matter is cooked in open containers at rising temperatures, the following processes usually occur in order, either sequentially or concurrently [3, 4]:

(i) Volatiles, including some water, evaporate at temperatures below around 100°C .

(ii) Any leftover water that has been absorbed in the polymer is pushed out at around 100°C or somewhat higher.

(iii) Many typical polymer compounds degrade between 100°C and 500°C degrees Celsius. Water, carbon monoxide CO, and/or carbon dioxide CO₂, as well as a vast range of organic molecules, are common decomposition products. Gases and volatile compounds leave the sample, and some may condense back into the smoke. In most cases, this procedure also consumes energy. Some volatiles has the potential to ignite and burn, resulting in a visible flame. The non-volatile residues often grow more carbon-rich and form big disordered molecules that range in color from brown to black. The substance is said to have been "charred" or "carbonized" at this stage.

(IV) If oxygen is not removed, the carbonaceous residue may begin to burn at $200 - 300^{\circ}\text{C}$, in a highly exothermic process with a minimal or little visible flame. The temperature rises spontaneously after carbon combustion begins, converting the residue into a blazing ember and producing carbon dioxide and/or monoxide.

(V) When the carbonaceous residue is completely burned, a powdery or solid mineral residue (ash) is frequently left behind, which is made up of inorganic oxidized minerals with a high melting point. Some of the ash may have been entrained by the gases as fly ash or particulate emissions during burning. The polymer continues to decompose endothermically until the reaction zone reaches the material's back-face, when the rest of the polymer is degraded to volatiles and char.

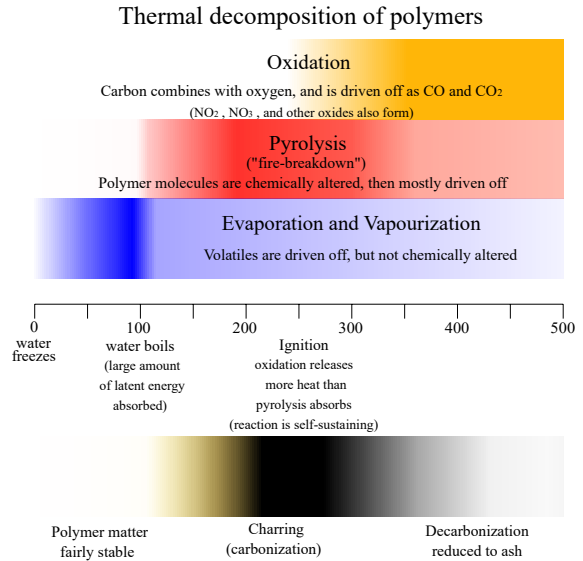


FIGURE 1. Processes in the thermal degradation of polymers.

In general engineering applications, the advent of Machine Learning (ML) and AI in recent years has provided an opportunity to construct quick surrogate ML models to replace classical FEM. Classic neural networks, on the other hand, map across finite-dimensional spaces and can thus only learn discretization-specific solutions. This is frequently a constraint in actual applications, necessitating the creation of mesh-invariant neural networks. The finite-dimensional operators and Neural-FEM are two popular neural network-based techniques for solving multiple PDEs [5, 6].

Neural-FEM. The third method is known as the physics-informed neural network (PINN). PINN differs from other machine learning paradigms widely employed for mechanics and physics challenges in terms of how data is needed and employed. Unlike supervised learning, which is often used for materials laws and requires artificial intelligence to be trained with labels in order to generate forecasts, the search for the solution in PINN does not require any data other than the ones required to form the loss function [7–11].

PINN challenges. The training of PINN, however, is far from simple. To construct the multi-layer perceptron, nonlinearities should be applied to each element of the output of the linear transformation. This is unlike the finite element method, which is a more entrenched framework with clear strategies and established mathematical analysis that guarantees convergence and stability for both the solution and weighting functions in pre-determined finite-dimensional spaces. Furthermore, for both forward and inverse problems, the physical constraints or controlling equations could be expressed in several ways; for instance, the collocation-based loss function, which evaluates the solution at specific collocation points, or the energy-based method that

can reduce the order of the derivatives in governing equations despite requiring numerical integrations. A large number of tunable hyperparameters, such as the configurations of the neural network, the types of activation functions, and the neuron weight initialization, as well as different techniques to impose boundary conditions while providing significant flexibility, may bewilder researchers who are unacquainted with neural networks [12–14].

Model and Method

- Heat Equation Thermal energy is transported into the polymer via thermal convection when the charring polymers are subjected to high-temperature loading. Decomposition of the resin will result in pyrolytic gases and solid leftovers. The polymer can be split into three zones based on the degree of pyrolysis of the polymer, as shown in Figure 1: (i) charring zone, in which the polymer entirely decomposes; (ii) pyrolysis zone, in which the polymer is disintegrating; and (iii) virgin material zone, in which the polymer has not yet begun to decompose [15].

In the thermal study of heat transfer in polymers, three main types of thermal energy transmission are often considered: conduction, convection, and radiation. However, for the sake of simplicity, all mathematical models for polymers cover the effect of heat conduction in the case of one-sided heating only. The effect of external convection on heat transfer is rarely explored. Similarly, heat radiation from a polymer is rarely taken into account. So, the following PDE governs heat transfer in polymers, i.e., heat transfer with internal heat generation is expressed as [16, 17].

$$\frac{\partial}{\partial t}(\rho C_p T) = \frac{\partial}{\partial x} \left(k_{xx} \frac{\partial T}{\partial x} \right) + \frac{\partial}{\partial y} \left(k_{yy} \frac{\partial T}{\partial y} \right) + \frac{\partial}{\partial z} \left(k_{zz} \frac{\partial T}{\partial z} \right) + \dot{Q}, \quad (1)$$

where T is the temperature, C_p , k , and ρ are the solid's specific heat capacity, conductivity, and density, respectively, and \dot{Q} is the rate of internal heat consumption. The change in thermal energy per unit volume is represented on the left-hand side of the equation, while the energy flux owing to conduction is represented on the right-hand side. The through-thickness direction is defined by the x-direction, whereas the planar directions are defined by the y- and z-directions.

Internal heat consumption in polymeric adhesives is expressed as a function of the degree of burning $\alpha \in (0, 1)$, which is a measure of the conversion achieved during the polymeric material's burning reactions. The relationship between \dot{Q} and α , in particular, can be expressed as [18, 19]

$$\dot{Q} = -Q_r \frac{d\alpha}{dt}, \quad (2)$$

where Q_r is the heat of reaction generated per unit mass of polymer during burning [20]. The evolving degree of burning in polymeric materials is usually controlled by an ordinary differential equation that indicates the rate of burning as a function of immediate temperature and degree of burning [21, 22].

$$\frac{d\alpha}{dt} = g(\alpha, T) > 0. \quad (3)$$

In the space-time domain (x, t) , this results in a coupled system of differential equations for temperature and degree of burning. The temperature $T(x, t)$ and degree of burning $\alpha(x, t)$ in the polymeric material are predicted by solving this system of differential equations with initial and boundary conditions. The aim of this research is to solve the system of differential equations for the polymeric system burning.

- PINN In the PINN methodology, network training takes place by minimizing the total loss of the network parameters Θ ,

$$\Theta^* = \underset{\Theta \in \mathbb{R}^D}{\operatorname{argmin}} \mathcal{L}_{\mathcal{F}}(\mathbf{X}; \Theta). \quad (4)$$

An error or loss function is defined in PINNs utilizing the network's processed outputs and derivatives based on the equations guiding the problem's physics. As a result, the network's total loss, $\mathcal{L}_{\mathcal{F}}$, is made up of the sum of loss terms for the PDE ($\mathcal{L}_{\mathcal{F}}$), and the initial and boundary conditions ($\mathcal{L}_{\mathcal{B}}$).

$$\mathcal{L}_{\mathcal{F}}(\Theta) = \mathcal{L}_{\mathcal{F}}(\Theta) + \mathcal{L}_{\mathcal{B}}(\Theta), \quad (5)$$

The loss caused by a mismatch with the governing differential equations \mathcal{F} is represented by the first term, $\mathcal{L}_{\mathcal{F}}$. It imposes the differential equation \mathcal{F} at collocation points over the domain, Ω , which can be chosen uniformly or unevenly. The other term, $\mathcal{B}(\hat{u}_{\Theta}) = g$, represents the loss caused to mismatch with the boundary or initial conditions. A mean square error formulation is used in a common implementation of the loss [23], where

$$\mathcal{L}_{\mathcal{F}}(\Theta) = \operatorname{MSE}_{\mathcal{F}} = \quad (6)$$

$$\frac{1}{N_c} \sum_{i=1}^{N_c} \|\mathcal{F}(\hat{u}_{\Theta}(z_i)) - f(z_i)\|^2 = \frac{1}{N_c} \sum_{i=1}^{N_c} \|r_{\Theta}(u_i) - r_i\|^2,$$

and

$$\mathcal{L}_{\mathcal{B}}(\Theta) = \text{MSE}_{\mathcal{B}} = \frac{1}{N_B} \sum_{i=1}^{N_B} \|\mathcal{B}(\hat{u}_{\Theta}(z_i)) - g(z_i)\|^2. \quad (7)$$

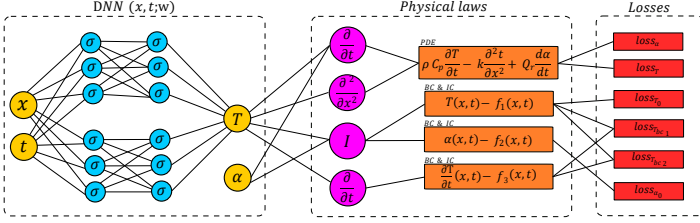


FIGURE 2. A schematic of PINN blocks. Differential equation residual (loss) terms, as well as initial and boundary conditions, make up PINNs.

Validation

Training and Hyperparameter Searches It is hardly surprising that network size and architecture, as well as optimizer hyperparameters like learning rate, can have a significant impact on PINN solution quality. We used the hyperbolic-tangent and sigmoid activation functions to create neural networks with four hidden layers and 20 neurons in each layer for all of the examples in this paper. We used the Adam optimizer with an initial learning rate of 2×10^{-3} and an exponential learning decay to 10^{-5} at the end of training. We have also explored a range of hyperparameters, but we have not noticed any substantial improvements in terms of improving the pyrolysis problem studied here. Fig. 3 shows the training history for various hidden layers and neurons.

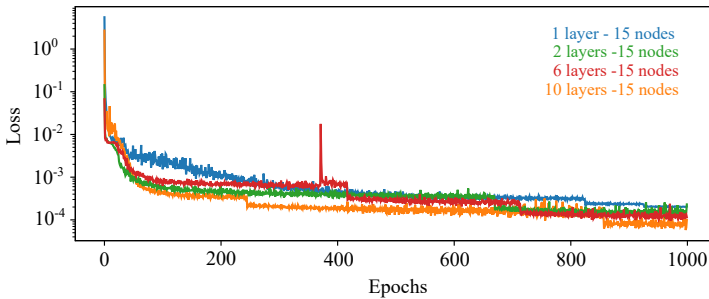


FIGURE 3. Losses for a variety of hidden layers.

Comparison with Numerical Results The reference numerical model results will be compared to the above-mentioned best-

performing PINN model outputs in this part. Fig. 4 shows the PINN, numerical solution, and errors. As you can see, the PINN solution has a high level of agreement with the expected solution when compared to the findings of numerical analysis. The upper face is given a temperature of $T_t = 700$, while the bottom face is given a temperature of $T_t = 700\sin(\frac{\pi}{20}t)$. $T_0 = 700x^3$ is the initial temperature.

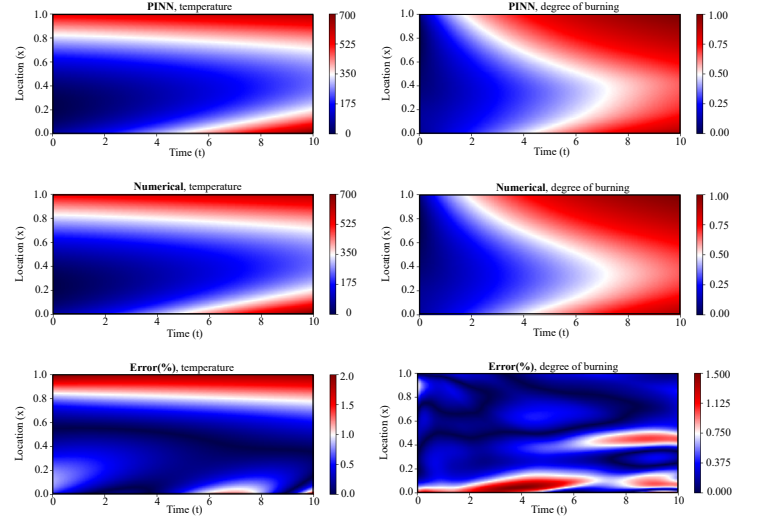


FIGURE 4. PINN and numerical predictions for full cycle of burning for temperature (left), and degree of burning (right).

CONCLUSION

In this paper, we studied a comprehensive study on Physics-Informed Neural Networks (PINNs) for the forward solution of pyrolysis problems by making the training more straightforward. We explored how Physics-Informed Neural Networks (PINNs) can be employed to solve pyrolysis problems in the forward phase. Our research is the first to explore fully coupled temperature-degree-of-burning relationships in pyrolysis problems. We presented a dimensionless version of these relations that leads to the optimizer's stable and convergent behavior.

While the achieved results are close to our expectations, it should be noted that training PINNs is time-consuming. We relate the training challenge to the multi-objective optimization issue and the application of a first-order optimization algorithm, as reported by others. Given the difficulties encountered and overcome in this work for the forward problem, the next step is to use PINNs to inverse burning situations.

REFERENCES

- [1] Natali, M., Puri, I., Rallini, M., Kenny, J., and Torre, L., 2016. "Ablation modeling of state of the art epdm based

- elastomeric heat shielding materials for solid rocket motors”. *Computational Materials Science*, **111**, pp. 460–480.
- [2] Chronopoulos, D., Ichchou, M., Troclet, B., and Bareille, O., 2013. “Thermal effects on the sound transmission through aerospace composite structures”. *Aerospace Science and Technology*, **30**(1), pp. 192–199.
- [3] Xu, Y., Lv, C., Shen, R., Wang, Z., and Wang, Q., 2019. “Experimental investigation of thermal properties and fire behavior of carbon/epoxy laminate and its foam core sandwich composite”. *Journal of Thermal Analysis and Calorimetry*, **136**(3), pp. 1237–1247.
- [4] Jebellat, E., Baniassadi, M., Moshki, A., Wang, K., and Baghani, M., 2020. “Numerical investigation of smart auxetic three-dimensional meta-structures based on shape memory polymers via topology optimization”. *Journal of Intelligent Material Systems and Structures*, **31**(15), pp. 1838–1852.
- [5] Kochkov, D., Smith, J. A., Alieva, A., Wang, Q., Brenner, M. P., and Hoyer, S., 2021. “Machine learning–accelerated computational fluid dynamics”. *Proceedings of the National Academy of Sciences*, **118**(21).
- [6] Ghaderi, A., Morovati, V., and Dargazany, R., 2021. “A bayesian surrogate constitutive model to estimate failure probability of elastomers”. *Mechanics of Materials*, **162**, p. 104044.
- [7] Bar, L., and Sochen, N., 2019. “Unsupervised deep learning algorithm for pde-based forward and inverse problems”. *arXiv preprint arXiv:1904.05417*.
- [8] Karniadakis, G. E., Kevrekidis, I. G., Lu, L., Perdikaris, P., Wang, S., and Yang, L., 2021. “Physics-informed machine learning”. *Nature Reviews Physics*, **3**(6), pp. 422–440.
- [9] Chen, W., Wang, Q., Hesthaven, J. S., and Zhang, C., 2021. “Physics-informed machine learning for reduced-order modeling of nonlinear problems”. *Journal of Computational Physics*, **446**, p. 110666.
- [10] Haghghat, E., Raissi, M., Moure, A., Gomez, H., and Juanes, R., 2021. “A physics-informed deep learning framework for inversion and surrogate modeling in solid mechanics”. *Computer Methods in Applied Mechanics and Engineering*, **379**, p. 113741.
- [11] Ghaderi, A., Morovati, V., Chen, Y., and Dargazany, R., 2022. “A physics-informed multi-agents model to predict thermo-oxidative/hydrolytic aging of elastomers”. *International Journal of Mechanical Sciences*, p. 107236.
- [12] Bhattacharya, K., Hosseini, B., Kovachki, N. B., and Stuart, A. M., 2020. “Model reduction and neural networks for parametric pdes”. *arXiv preprint arXiv:2005.03180*.
- [13] Psaros, A. F., Kawaguchi, K., and Karniadakis, G. E., 2021. “Meta-learning pinn loss functions”. *arXiv preprint arXiv:2107.05544*.
- [14] Fuhg, J. N., Böhm, C., Bouklas, N., Fau, A., Wriggers, P., and Marino, M., 2021. “Model-data-driven constitutive responses: application to a multiscale computational framework”. *International Journal of Engineering Science*, **167**, p. 103522.
- [15] Dennis, C., and Bojko, B., 2019. “On the combustion of heterogeneous ap/htpb composite propellants: A review”. *Fuel*, **254**, p. 115646.
- [16] Bogetti, T. A., and Gillespie Jr, J. W., 1992. “Process-induced stress and deformation in thick-section thermoset composite laminates”. *Journal of composite materials*, **26**(5), pp. 626–660.
- [17] Tadini, P., Grange, N., Chetehouna, K., Gascoin, N., Senave, S., and Reynaud, I., 2017. “Thermal degradation analysis of innovative pekk-based carbon composites for high-temperature aeronautical components”. *Aerospace Science and technology*, **65**, pp. 106–116.
- [18] Mouritz, A., and Gibson, A., 2006. “Modelling the thermal response of composites in fire”. *Fire properties of polymer composite materials*, pp. 133–161.
- [19] Mouritz, A., Mathys, Z., and Gardiner, C., 2004. “Thermo-mechanical modelling the fire properties of fibre–polymer composites”. *Composites Part B: Engineering*, **35**(6-8), pp. 467–474.
- [20] Henderson, J., and Wiecek, T., 1987. “A mathematical model to predict the thermal response of decomposing, expanding polymer composites”. *Journal of composite materials*, **21**(4), pp. 373–393.
- [21] Henderson, J. B., Wiebelt, J. A., and Tant, M., 1985. “A model for the thermal response of polymer composite materials with experimental verification”. *Journal of composite materials*, **19**(6), pp. 579–595.
- [22] Gibson, A., Wright, P., Wu, Y.-S., Mouritz, A., Mathys, Z., and Gardiner, C., 2003. “Modelling residual mechanical properties of polymer composites after fire”. *Plastics, Rubber and Composites*, **32**(2), pp. 81–90.
- [23] Shahbandegan, S., and Naderi, M., 2021. “Multiswarm binary butterfly optimization algorithm for solving the multi-dimensional knapsack problem”. In 2021 29th Iranian Conference on Electrical Engineering (ICEE), IEEE, pp. 545–550.